UNCLASSIFIED

AD NUMBER

AD243582

NEW LIMITATION CHANGE

TO

Approved for public release, distribution unlimited

FROM

Distribution authorized to U.S. Gov't. agencies and their contractors; Administrative/Operational Use; 15 Sep 1960. Other requests shall be referred to Office of Naval Research, 800 North Quincy Street, Arlington, VA 22217-5660.

AUTHORITY

ONR ltr, 28 Jul 1977

THIS PAGE IS UNCLASSIFIED

REPORT NO. 56

BURNING VELOCITIES OF THE HYDROGEN PEROXIDE DECOMPOSITION FLAME

Prepared for the
Office of Naval Research
Contract Nonr 1841 (11)
NR-092-008

BY

Charles N. Satterfield
Ephraim Kehat

Oct 4 1960

Reproduction in Whole or in Part is Permitted for any Purpose by the United States Government

423200

MASSACHUSETTS INSTITUTE OF TECHNOLOGY
Department of Chemical Engineering Cambridge, Mass.

60-4-5
XEROX

Division of Sponsored Research, Project 7476
Sept. 15, 1960

REPORT NO. 56

BURNING VELOCITIES OF THE HYDROGEN PEROXIDE DECOMPOSITION FLAME

Prepared for the
Office of Naval Research
Contract Nonr 1841 (11)
NR - 092 - 008

BY

Charles N. Satterfield
Ephraim Kehat

MASSACHUSETTS INSTITUTE OF TECHNOLOGY
Department of Chemical Engineering Cambridge, Mass.

Division of Sponsored Research, Project 7476
Sept. 15, 1960

BURNING VELOCITIES OF THE HYDROGEN PEROXIDE DECOMPOSITION FLAME

by

Charles N. Satterfield
and
Ephraim Kehat

Abstract

Burning velocities of the hydrogen peroxide decomposition flame have been measured by the bunsen burner method at pressures between 0.5 and 1 atmosphere. The flame reaction follows approximately first order kinetics with an activation energy of 35 kcal/mole, and shows general agreement with the mechanism and kinetics of the homogenous non-flame reaction. A single plot of the logarithm of the product of the square of the burning velocity and the pressure versus the reciprocal flame temperature correlated the data obtained here at all pressures and also burning velocities above liquid solutions of H_2O_2. This covers a 200-fold range of burning velocity. The burning velocity was also corelated with quenching distance and some approximate blow-off and flash-back limits are also given.

The object of this investigation was to measure burning velocities of decomposition flames of hydrogen peroxide-water vapor mixtures, as a function of concentration and pressure, as a means of studying the mechanism of this reaction in the flame and comparing it to the mechanism of the non-flame reaction. The homogenous decomposition reaction has become much better understood recently (9, 19) and it was hoped that because of the relative simplicity of this reaction compared to those occurring in almost any other flame, it would be possible to relate burning velocity theories to the homogenous reaction mechanism and actual burning velocity measurements.

The burning rates and other characteristics of the decomposition flame above aqueous hydrogen peroxide solutions have been recently published (32). The only other study of flame velocities in hydrogen peroxide vapor was that reported in the Sc.D. thesis by Ceckler (4) who did the pioneering work and obtained some preliminary data.

PROCEDURE

Flame velocities were determined by the bunsen burner method, using shadow photography. Since hydrogen peroxide solutions and vapor decompose to some extent on all surfaces, particular care must be taken to choose proper materials of construction and methods of cleaning (34, 36). At one atmosphere pressure, temperatures of

130-150° C and above and concentrations above about 70 wt % for the liquid and over 26 mole % for the vapor, spontaneous ignition of a flame in the vapor or above the solution can readily occur.

In the present apparatus the hydrogen peroxide solution and vapor were allowed to come in contact only with specially treated Pyrex surfaces. The equipment was soaked in boiling detergent solution for an hour or more, rinsed with tap water and then with distilled water and soaked in a hot solution of concentrated 3:1 sulfuric and nitric acid mixture for 24 hours. This treatment is believed to leach most of the heavy metal ions from the surface. The equipment was then rinsed in conductivity water, great care being taken to exclude dust and dirt in this stage. All openings were securely covered in aluminum foil and the equipment was placed in an annealing oven. The termperature of the oven was raised to 510° and kept there for five minutes. The furnace was then shut off and the equipment was allowed to cool slowly in it for three hours. Five minutes was considered an optimal period, long enough to allow some closing of the pores created in the leaching process, and yet not long enough for appreciable diffusion of heavy metal ions from the interior of the glass to the surface.

The equipment thus cleaned could be used for two or three runs. If a flame occurred in the equipment, it had to be retreated before reuse, because the flame temperatures of about 1000°C change the nature of the surface. After fifteen to twenty treatments glassware had to be replaced due to overetching of the treated surfaces or partial devitrification from the many annealings.

The apparatus is shown in Figure 1. The hydrogen peroxide vapor was generated from a batch evaporator, initially containing 750 cc of concentrated H_2O_2 solution. Boiling rates were 2 - 4.5 gm/min, and were controlled by the heat input to the vaporizer flask. The vapor was superheated by 2 - 3 degrees Centigrade and then passed into a 5 mm. i.d. 30 cm. long Pyrex burner tube that was kept at a constant temperature. During start-up, the top of the burner tube was connected to a condenser and samples of the vapor were taken by condensing all the generated vapor into a series of sample beakers placed on a revolving tray. After equilibrium was established, the connecting tube was removed and a hot wire was positioned over the burner tube to ignite the vapor. The last two or three samples, obtained after equilibrium had been achieved, were weighed and analyzed. From a knowledge of the time during which each beaker's contents were collected and the analysis, the flow rate and composition were calculated.

The concentration of the vapor increased 0.1 - 0.2 weight percent per minute as the vaporization proceeded. Only a few minutes elapsed in most runs from the last sample to the blowing out of the flame. Therefore extrapolation of the concentration from the last sample to the

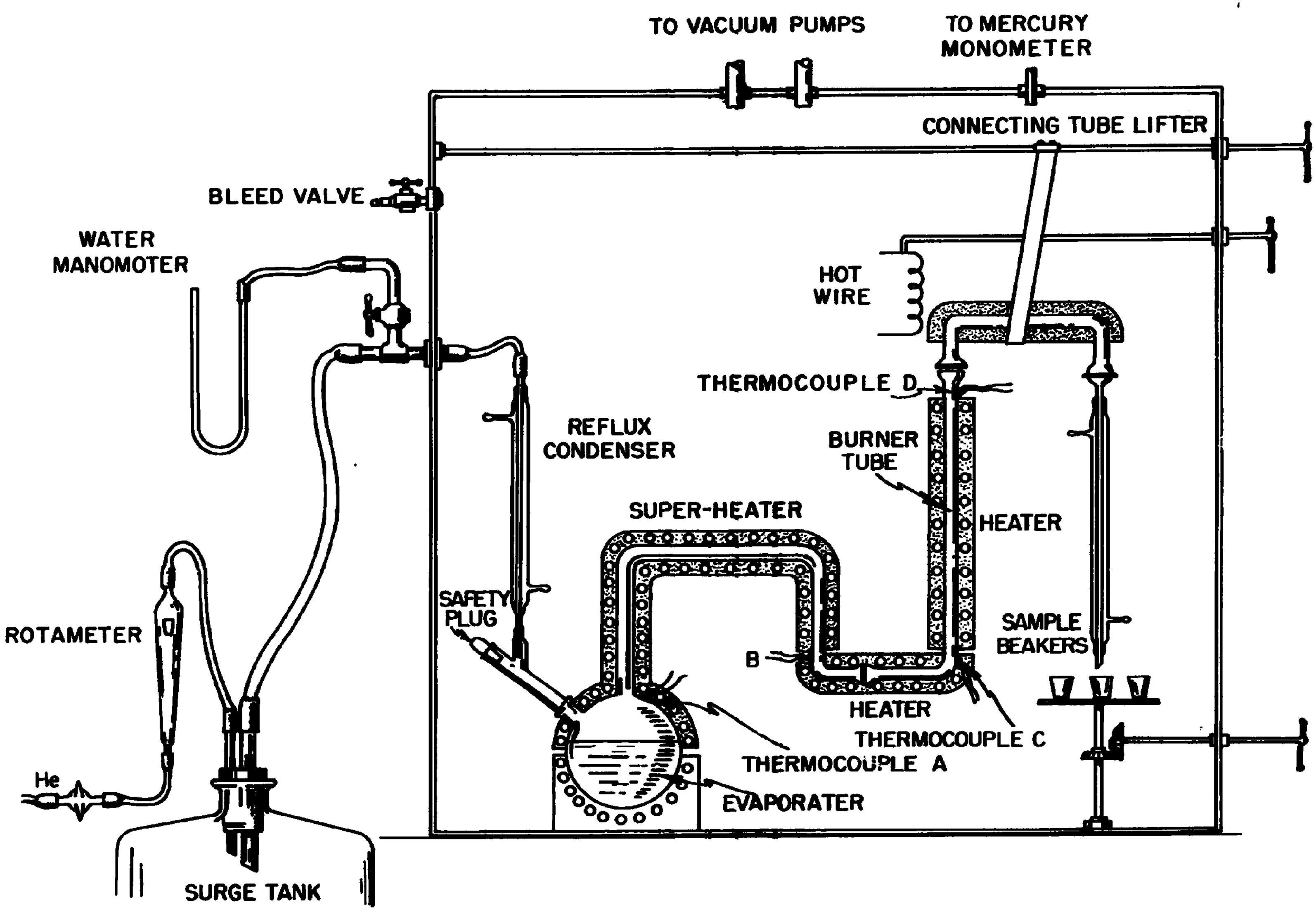

FIG. I SCHEMATIC DIAGRAM OF APPARATUS

time the pictures were taken involved only a small correction.

Four thermocouples were used for temperature control, located as shown in Figure 1. In a number of calibrating runs, temporary thermocouples were placed in one inch long Pyrex inserts inside the bottom and top of the burner tube, in order to establish the proper heating rates and permanent thermocouple settings to insure that the vapor was kept at the same temperature at the bottom and top of the burner tube.

The evaporator flask was heated by a 400 watt Thermowell shell heater, the superheaters by Electrothermal heating tapes. The burner tube was heated by surrounding it with a copper tube wound with Chromel A resistance wire. All connections were made with ball and socket clamped joints. The top of the burner tube was also a ball joint ground down to eliminate the lip originally present.

The evaporator was connected through a reflux condenser to a manometer and surge tank, both of which were used only at atmospheric pressure. Helium was fed into the evaporator and the rest of the system during warm-up to help distribute heat to the Pyrex walls more evenly, and at the end of a run to blow off the flame. No helium was used during sampling or establishment of the flame.

The whole assembly was contained in a large pressure-tight box, equipped with windows and a detachable back plate, in which a partial vacuum could be maintained. The optical system was a two watt concentrated arc lamp, a lens that changed the light into a parallel, slightly divergent beam, and a ground glass plate on which the image was cast. This was photographed by a reflex camera with a close-up lens attachment. The best usable pictures were obtained with underexposed fine grain film and high contrast developing.

RESULTS

Studies were made at 1, 0.72 and 0.5 atmospheres. Experimental and calculated results are shown in Table II (Appendix) and the burning velocities are plotted as a function of vapor concentration in Figure 2.

The vapor temperature in each case was 2-3°C above the boiling temperature of the solution in equilibrium with the vapor concentration. The flame temperature was taken to be equal to the adiabatic decomposition temperature. As a test of this assumption Mendes (27) found with a thermocouple probe only a 10°C difference between calculated and measured flame temperatures in one of her runs. Molal heat capacities of the products were taken from Perry (29 p 222). The heat of decomposition of hydrogen peroxide in the temperature range in this work, i.e. 390-420°C is 25250 ± 5 cal/mole (36 p. 251).

The vapor velocity was calculated from the mass evaporating rate measured by the last three samples in

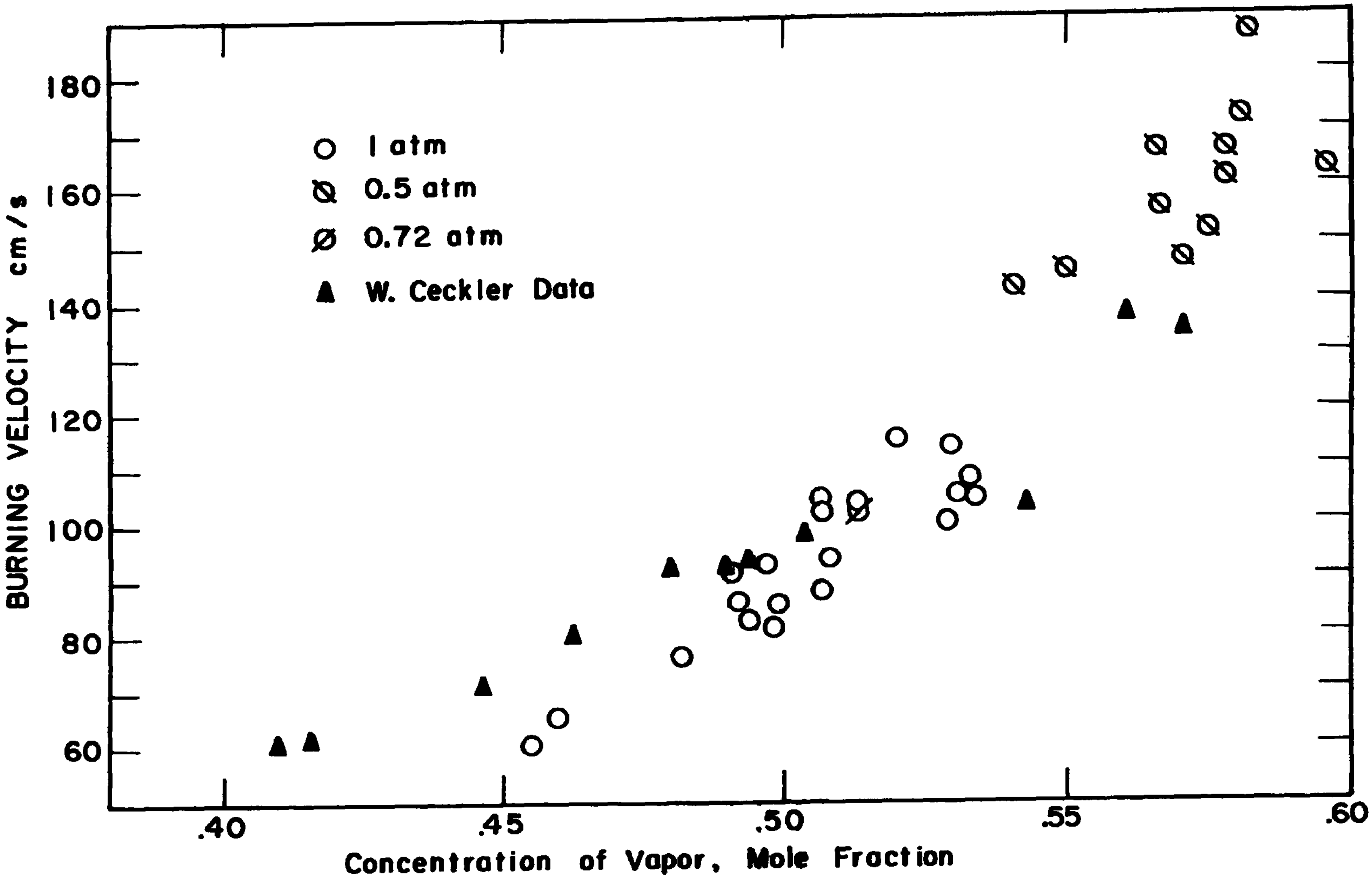

FIG. 2 EFFECT OF VAPOR CONCENTRATION ON BURNING VELOCITY

each run and the concentration of the vapor, assuming ideal gas behaviour at these temperatures. Vapor velocities ranged from 245 to 613 cm/sec. The useful range for any composition was determined by the flashback and blow-off limits.

The burning velocity is defined at the inner boundary of the flame, which is represented by the outer boundary of the flame shadow (12, 17). The burning velocity was calculated from measurements of the outer boundaries of the flame shadow by the method of Clingman and Pease (5). This method gives a single average value for the burning velocity over most of the flame front by taking into consideration the laminar distribution of vapor velocity.

A careful check of each point in Figure 2 showed no correlation whatsoever between vapor velocity and burning velocity. This is consistent with the general behaviour of bunsen burner flames (6, 11, 14).

Because of the fuzzy definition of the outer edge of the shadow, it was necessary occasionally to make more than one tracing of the edge of the shadow from the same picture. Each point in Figure 2 represents the average of measurements of three to six pictures from the same run. The scatter in the data is due mostly to the subjective inaccuracies in tracing the outer outline of the shadow, inherent in the shadow method. Only 2/5 to 2/3 of the flame periphery was used in each picture, as the shape of the flame is distorted at the base of the flame from the quenching effect of the burner tube rim. The shape of the flame tip is also distorted by the thermal effects from the increased ratio of flame area to vapor volume in that region, and by minute fluctuations of the vapor flow, which are exaggerated at the tip.

Runs where the vapor flow had not reached steady state, where analysis of subsequent samples showed a decrease instead of a slight increase in concentration and where the pictures showed the arc lamp was not in the same horizontal plane as the top of the tube, were discarded. In some low pressure runs the flames were not stable because of slight pressure variations. The flame passed through a cycle lasting from ten seconds to five minutes. At the lowest vapor velocity the flame stabilized, then it increased slightly in size and fluctuated mildly for most of the cycle. Finally it increased greatly in size and blew off. Only pictures from the middle of the cycle were used in such cases.

The ratio of length to diameter of the burner tubes was sixty. The temperature of the vapor flowing in the tube was kept constant within 1°C. The Reynolds numbers ranged between 700 and 1400. It seems reasonable to assume that a laminar flow was established at the exit of the burner tube. In the flame cone the flow pattern is distorted and local vapor velocities are changed by 5 - 15% (39). However, Fristrom (11) and Lewis and Von Elbe (23) have shown that this does not appreciably affect the measured burning velocity.

This is also indicated by the usually straight lines obtained in this work by the Clingman and Pease correlation. This correlation assumes a laminar flow distribution and would have been affected by a change in the flow pattern.

The lower limit of concentration that could be studied at each pressure was dictated by quenching effects and by the narrow range of velocities between flashback and blow-off. The upper limit of concentrations was enforced by the invariable adventitious ignition of the solution in the vaporizer flask at liquid concentrations of about 90% wt. or above.

Physical properties were calculated from the following sources:

Thermal conductivity: Only properties of the final products, H_2O and O_2, were used in the correlations. For water, the equation of Keyes (22) is valid up to 823°K. It checked with the Bureau of Standards value (18) at 800°K and was used up to 1600°K. For oxygen, the equation of Keyes (21) is valid up to 375°K. It checked within 2% at 1000°K and within 8% at 2000°K with the values calculated by Baulknight (2) and was used up to 1600K. For mixtures, the method of Bromley as outlined in Reid and Sherwood (31) was used for the calculation of thermal conductivity of mixtures.

Molal Heat Capacity: Molal heat capacities were taken from the National Bureau of Standards tables (18) and the values for mixtures were combined on a molar basis.

Viscosity: Viscosity data for H_2O and O_2 were taken from the National Bureau of Standards tables (18). Viscosities of H_2O_2 / H_2O mixtures were calculated from the experimental results of Satterfield and co-workers (35).

The Homogeneous Decomposition Reaction

The decomposition of hydrogen peroxide vapor is catalyzed by most surfaces. Even in the most inert reactors, it is necessary to go to substantially elevated temperatures (above 400°C) before the rate of the homogeneous reaction exceeds that on the reactor surface at partial pressures of the order of 1 - 10 mm. of mercury.

In the past eleven years five studies have been published on the homogeneous, non flame, decomposition of hydrogen peroxide vapor (9, 15, 19, 26, 33). Early uncertainties over the mechanism of the reaction seem to have been resolved by the similar results of the two recent extensive independent studies by Hoare and co-workers (19) and Forst (9). At concentrations of the order of 0.1 to 22 millimeters of mercury and temperatures of 400 to 600°C, the mechanism is apparently as follows:

Initiation $H_2O_2 + M' \longrightarrow 2\ OH + M'$ (1)

Propagation $OH + H_2O_2 \longrightarrow H_2O + HO_2$ (2)

Termination $HO_2 + HO_2 \longrightarrow H_2O_2 + O_2$ (3)

or $HO_2 + OH \longrightarrow H_2O + O_2$ (4)

The overall rate expression fits the form:

$$\frac{d(H_2O_2)}{dO} = k(H_2O_2)(M') \qquad (5$$

Here (M') is a combination of concentrations and efficiencies of collision in the initiating step for all species present. The collision efficiencies reported by Hoare and co-workers (19), relative to a collision efficiency of unity for H_2O_2, are 0.73 for H_2O and 0.12 for O_2. Mr. R. Yeung of these laboratories has recently recalculated the data from all the reported studies of the homogenous decomposition of H_2O_2 and found that the best value for the activation energy from all the data is 44 Kcal/mole.

To illustrate the significance of the M' term, Table I shows how the value of (M') is calculated to change as the decomposition reaction proceeds. This is based on (M') = 1 for $y_o' = 1$, and shows values for initial H_2O_2 mole fractions of 0.45 and 0.60.

Table I

Change in (M') With Degree of Decomposition

Initial Mole Fraction of H_2O_2 (y_o')	Degree of Decomposition	Moles H_2O_2 Present Per One Mole of Initial Mixture, n	(M')
0.45	initial	.45	.852
	half reacted	.225	.723
	fully reacted	0.0	.618
0.60	initial	.60	.892
	half reacted	.30	.721
	fully reacted	0.0	.590

Table I shows that for a 100% change in concentration of H_2O_2, i.e. over the complete reaction, (M') changes by less than 35% and the per cent change is only slightly effected over the initial concentration range of 0.45 mole fraction H_2O_2 to 0.60. This in effect means that the overall reaction rate is more nearly first order than second order with respect to hydrogen peroxide concentration.

FLAME PROPAGATION THEORIES

From the formulation of the equations of flame propagation by von Karman and Penner (41) for similar boundary conditions, the following relationship is obtained:

$$\frac{S^2 P}{T_o} \quad \frac{C_p}{\lambda_f} \propto \left(\frac{P}{T_f}\right)^n \qquad (6)$$

The derivation of equation 6 is based on an eigenvalue which is constant if the preflame conditions are not varied. This condition is not met by the data of this work and the correlation, as expected, was not successful. However, this expression can be written for an explicit reaction order thus:

$$\underline{n = 1} \qquad \frac{S^2 P \, \overline{C_p}}{T_o^2 \, \lambda_f} = \frac{a}{T_f} \qquad (7)$$

$$n = 2 \qquad \frac{S^2 T_f \, \overline{C_p}}{T_o^2 \, \lambda_f} = \frac{b}{T_f} \qquad (8)$$

Where a and b are constants.

Table III (in appendix) presents the flame velocity data calculated in the forms of equations 7 and 8. Equation 7 gave the correlation in Figure 3. Equation 8 gave no correlation whatsoever.

The significance of Figure 3 is not in the linear relationship which may be partly due to the scatter in the data, but in the fact that flame velocities at both 0.5 and 1 atmosphere fell on the same curve.

For systems where concentrations and temperatures are held constant equation 6 is simplified to:

$$S \propto p^{(n/2)-1} \qquad (9)$$

However, since most flame reactions do not have a precise first or second order relationship, attempts to use this expression to predict the order of flame reactions, with the notable exception of the hydrazine decomposition flame (16), have not been successful. In general the pressure exponent has been found to vary between +0.2 and -0.5. Manton and Millikan (24) in their study of a large variety of hydrocarbons, found that the pressure exponent was a function of the burning velocity. The form of equation 7 indicates that for the hydrogen peroxide decomposition flame, the pressure dependence is approximately that predicted by equation 9 for a first order reaction.

The most widely used of the flame propagation theories is Semenov's thermal theory (37), principally because of the integrated form of his equations which is easy to apply in the correlation of burning velocity

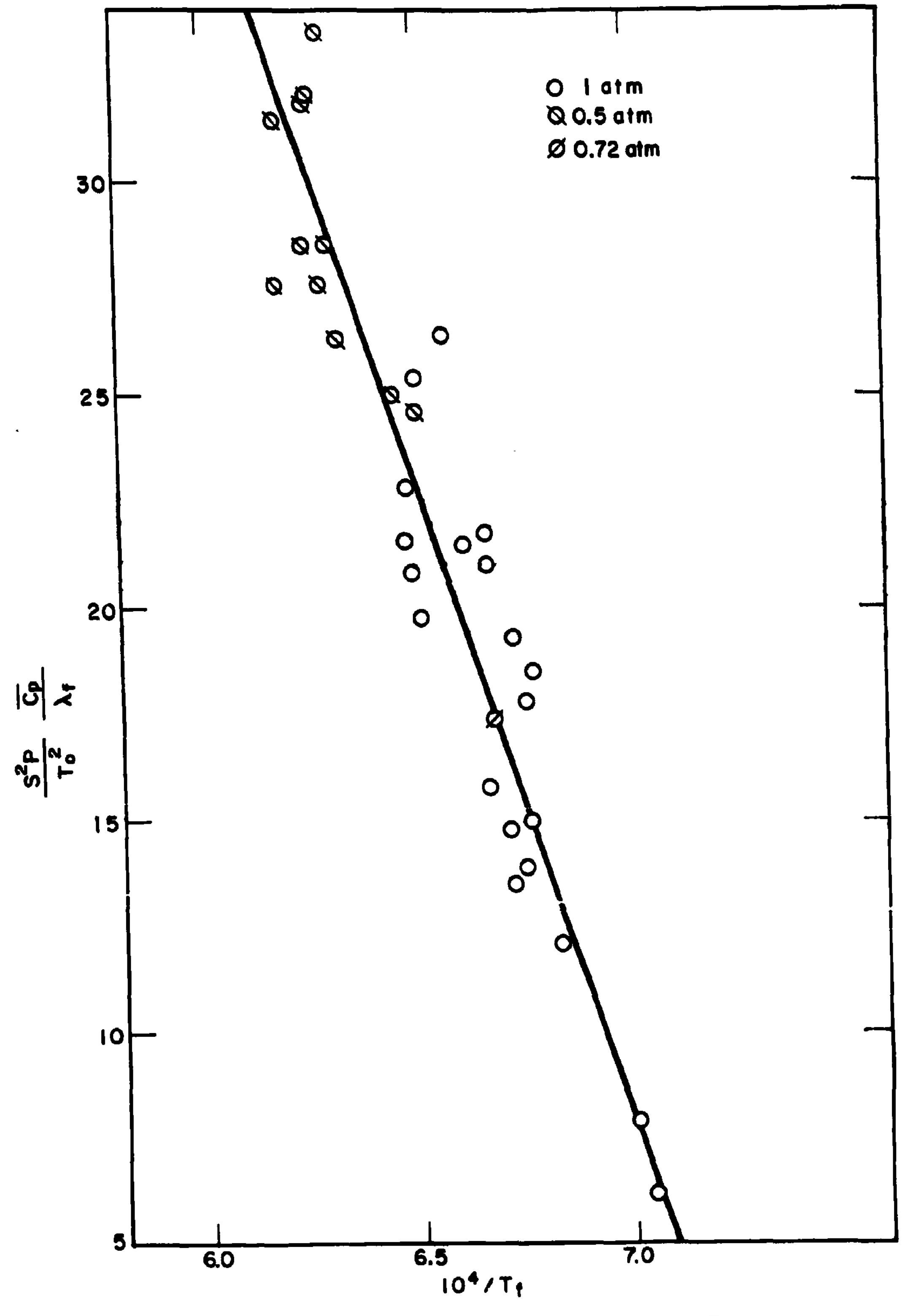

FIG. 3 CORRELATION OF DATA BY EQUATION 7

data with any other property of the combustible system. The Semenov equations for a flame reaction of first or second order can be written in the forms:

$$\text{First order} \quad \frac{S^2P \qquad y'^2}{T_f^3\, T_o^2\, \lambda_f C_{p_f}\, (2+y')} = k'\, e^{-\frac{E}{RT_f}} \qquad (10)$$

$$\text{Second order} \quad \frac{S^2 \qquad y'2}{T_f^4\, T_o^2\, \lambda_f C_{p_f}\, (2+y')^2} = k'\, e^{-\frac{E}{RT_f}} \qquad (11)$$

The present data were calculated in the form of equations 10 and 11 and are presented in Figures 4 and 5. It can be easily seen that the first order form correlates the data well, whereas the second order form shows a distinct trend to form a different line for each pressure. These facts strongly support the conclusion that the reaction is effectively first order and that the pressure effect is that predicted for a first order reaction.

The activation energy calculated from Figure 4 is 35 kcal/mole as compared with 44 kcal/mole for the homogeneous reaction at lower temperature.

A simplified expression of the Semenov equation, by neglecting pure thermal and transport effects, assumes the form:

$$S^2P = k\, e^{\frac{-E}{RT_f}}$$

Figure 6 is a plot of S^2P against the reciprocal of the flame temperature. This plot shows greater scatter than Figure 4, but an "apparent" activation energy calcu-

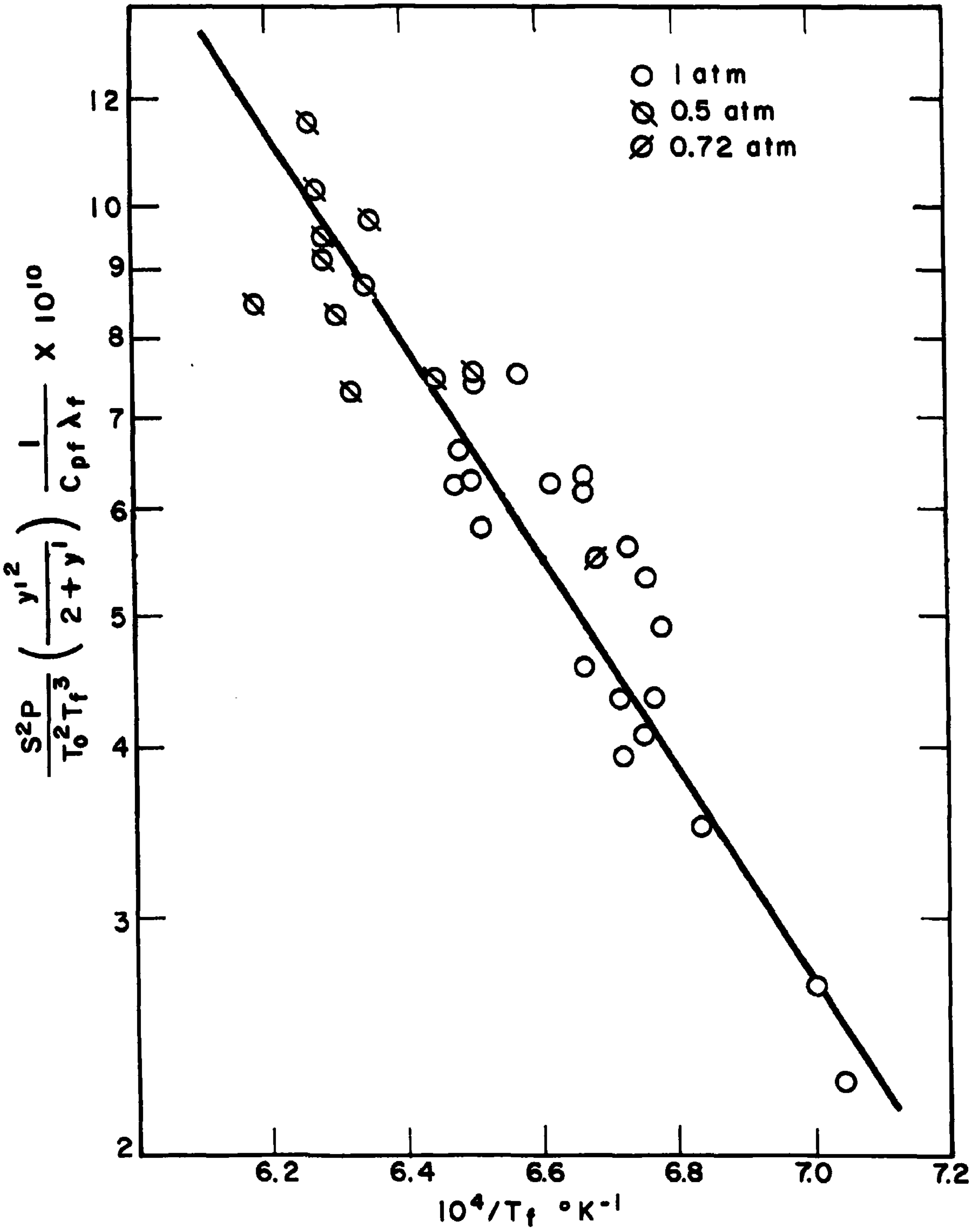

FIG. 4 CORRELATION OF DATA BY SEMENOV'S FIRST ORDER EXPRESSION

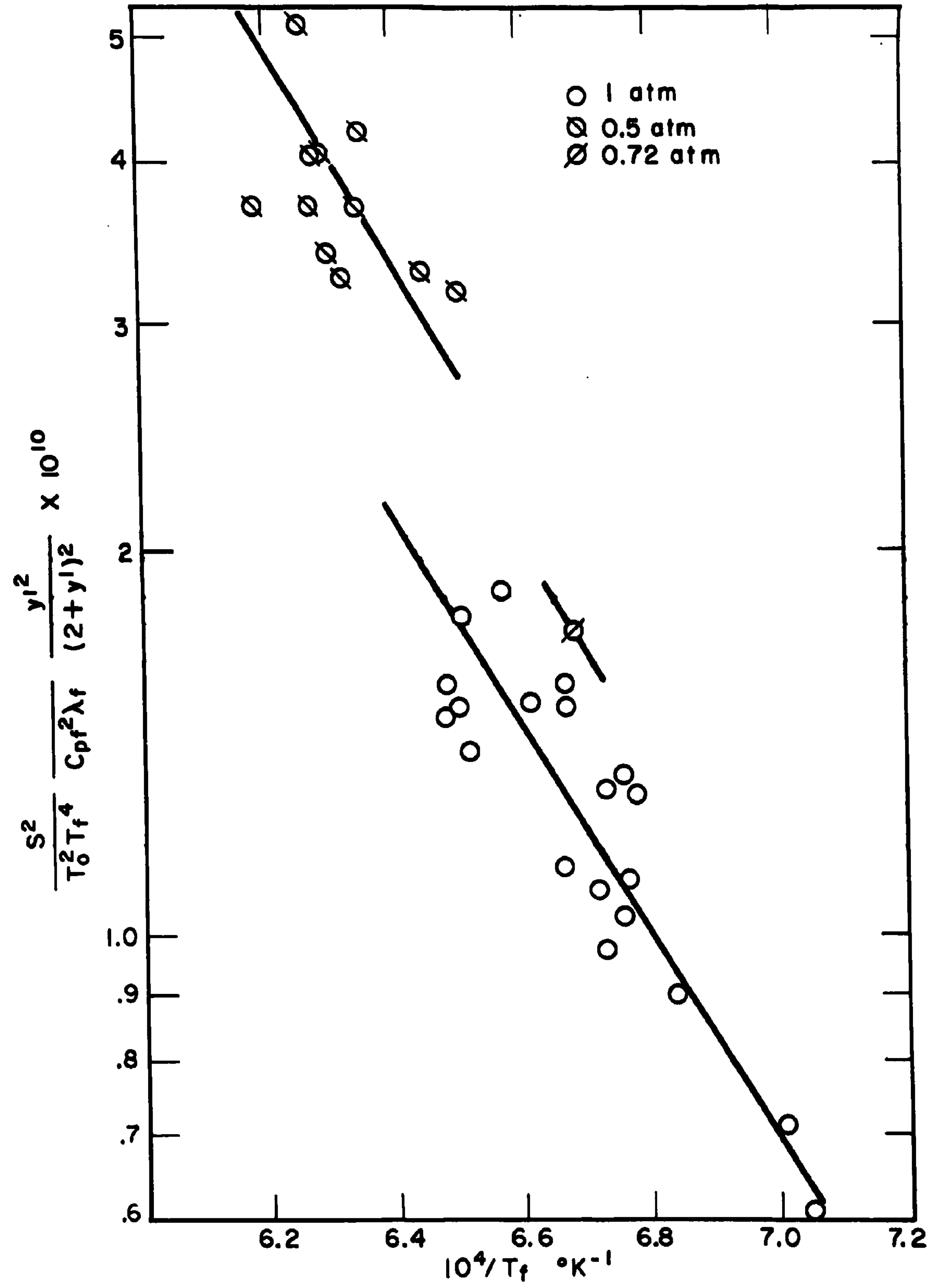

FIG. 5 CORRELATION OF DATA BY SEMENOV'S SECOND ORDER EXPRESSION

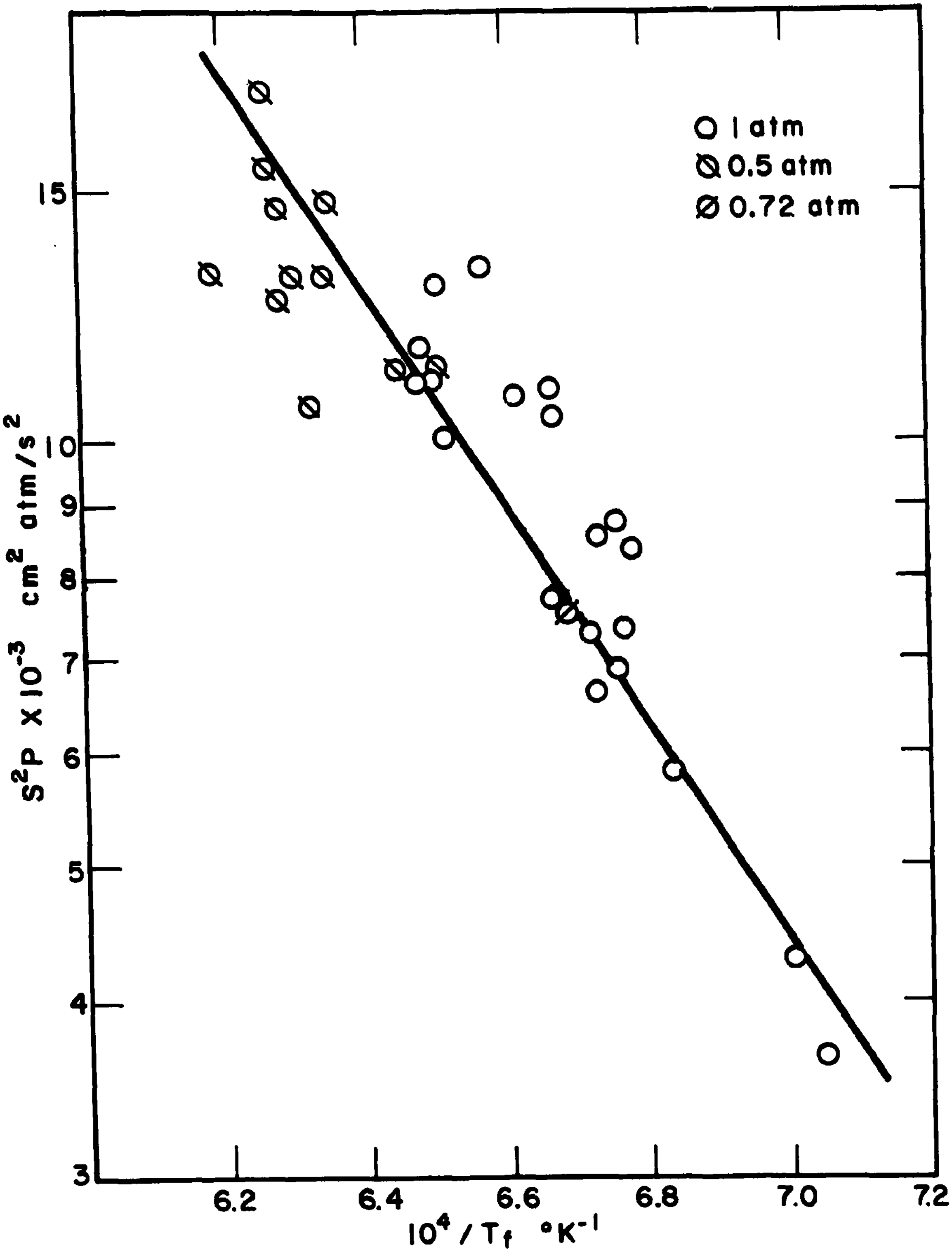

FIG. 6 SIMPLIFIED FIRST ORDER CORRELATION OF DATA

lated from the slope is also 35 kcal/mole. This conforms with the conclusions of Gerstein and co-workers (13) and Kaskan (20) that the most important factor in determining the burning velocity is the rate of reaction and that thermal and transport properties play a secondary role.

Activation energies for all types of flame reactions have been observed to have lower values than activation energies reported for the same reactions, believed to be taking place in the flames, when studied at much lower temperatures. This has reported for a large variety of hydrocarbon-oxygen-nitrogen flames (8, 28), for hydrogen-nitric acid flames (40), for the ethylene oxide decomposition flame (10) and for the hydrazine decomposition flame (16). There are also theoretical reasons why the activation energy should decrease with increase of reaction temperature. For example, Shuler (38) in his summary on gas phase reactions at high temperatures discusses (38) the effect of the non-equilibrium distribution of energy for exothermic high temperature reactions. Arrhenius type rate expressions assume an equilibrium distribution of energy. At high temperature and high rates of generation of energy, this equilibrium is not obtained, i.e. some molecules have more energy than predicted by the Arrhenius theory and consequently require less "activation" energy in order to react.

The change of (M') as the reaction proceeds, for different initial concentrations, follows parallel curves.

A correction factor (M') for the second order term, based on initial conditions, should apply throughout the reaction in the flame, for the effect of changes in initial concentration of H_2O_2. Such a correction factor (M') was calculated (Table VI) and the Semenov first order equation 6 as corrected by the second order term (M') is replotted in Figure 7. The spread of the data is slightly less than in Figure 4 and the calculated activation energy is 36 kcal/mole, only slightly changed. It is apparent that burning velocity is not a sensitive enough parameter for a study of the finer points of reaction mechanism in the flame.

CORRELATION OF BURNING VELOCITIES ABOVE LIQUID AND THOSE IN VAPOR

Mendes (27, 32) studied the burning rates of H_2O_2 solutions in tubes of 1.5 and 3.0 cm i.d. at concentrations of 71 - 97% weight and 0.13 - 1 atmospheres. She measured the rate of drop of liquid level under the flame and calculated burning velocities from the mass burning rates by assuming that the liquid vaporizes at the liquid temperature and then burns, and that the flame front is essentially flat.

Mendes' data were recalculated here in the form of Semenov's first order equation (equation 10) and in the S^2P form (Table IV). A plot of the logarithm of the product of the square of the burning velocity and the pressure against the reciprocal flame temperature for these data is shown in

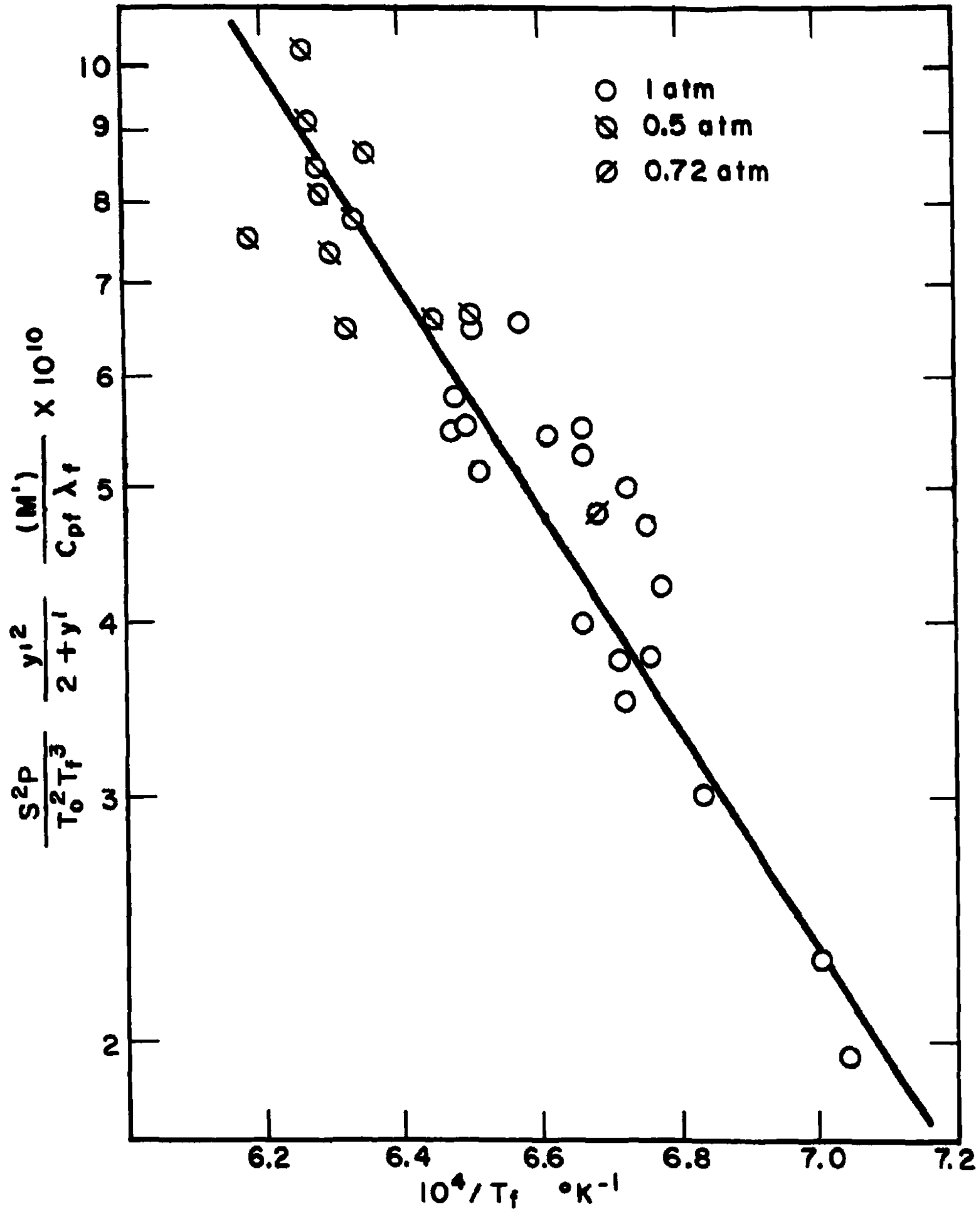

FIG. 7 SEMENOV'S FIRST ORDER CORRELATION OF DATA CORRECTED FOR EFFECT OF (M)

Figure 8. The continuation of the line from the similar plot of the data of this work (Figure 7), which is replotted in this figure, also correlates the data for burning velocities above liquid H_2O_2 solutions.

This is remarkable in view of the quenching effects and the heat losses typical of flames above liquid solutions (16). However, such studies have usually used small diameter tubes in which the flame and the hot liquid are enclosed by, and close to the tube walls all the time. Heat losses and quenching of radicals at the walls are considerable. In bunsen burner type flames for gaseous systems, only a small area at the base of the flame comes in contact with a wall. However, Mendes used large diameter tubes in her study and heated the tubes on the outside while taking the data, thereby minimizing the quenching effects and heat losses.

The data for all pressures is also correlated by the line in Figure 8. Two groups of data points deviate markedly from the average line. One group is at concentrations of .95 mole fraction and higher. ($10^4/T$ = about 7.5 on Figure 8. It has been shown previously (32) that the scatter of these data was associated with variations in the circulation pattern of the liquid hydrogen peroxide solution. For runs at liquid temperatures the furthest below the boiling point, a sharp interface was observed about 3 mm below the surface. The top layer presumably consisted of less dense solution and probably

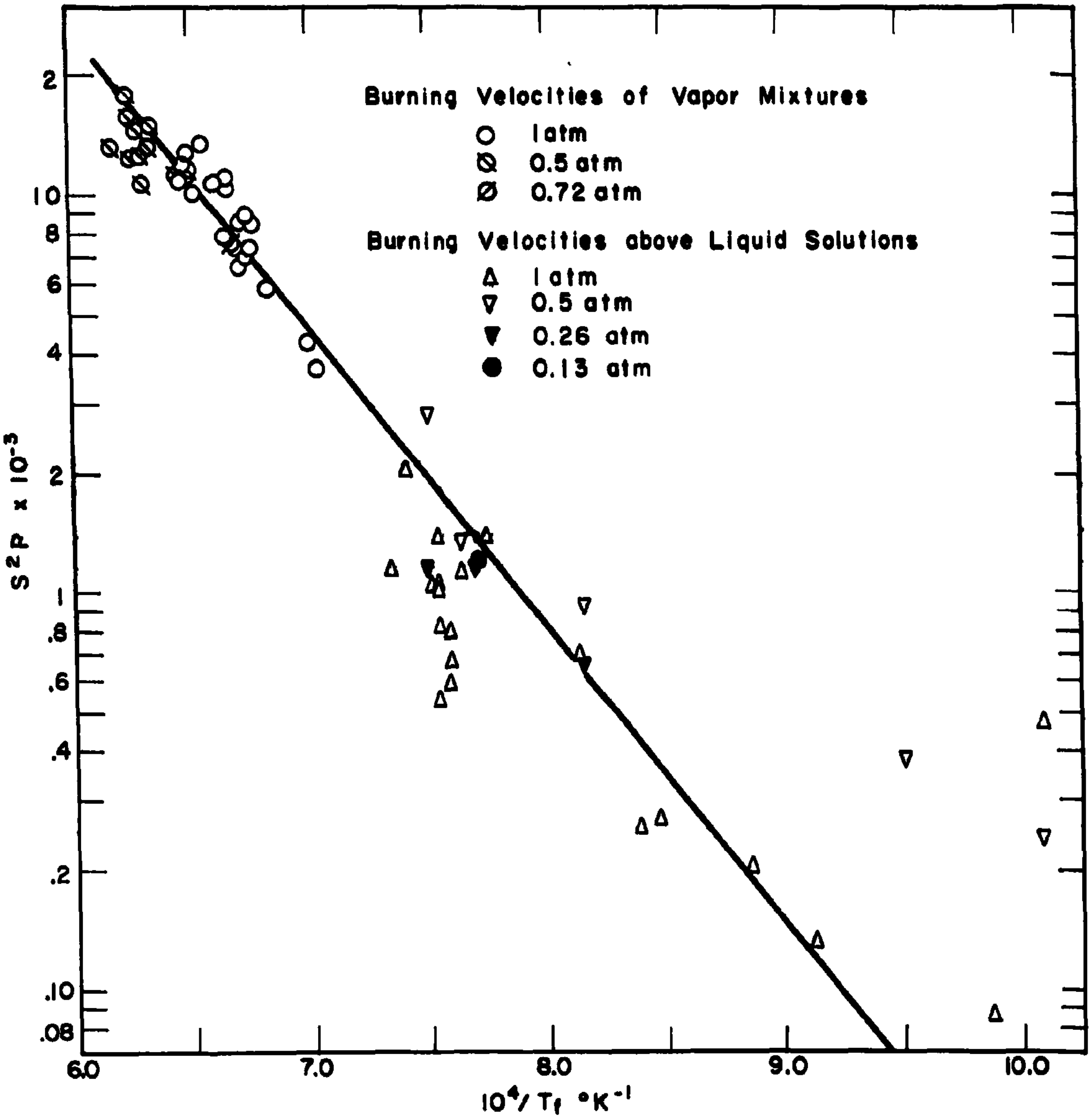

FIG. 8 CORRELATION OF BURNING VELOCITIES OF VAPOR MIXTURES AND LIQUID SOLUTIONS OF H_2O_2

lower concentration than that reported which was based on a sample removed from the bottom of the tube.

The second deviating group consists of four points at the lower right hand portion in which H_2O_2 concentration was substantially lower than that for other runs at the corresponding pressure and very close to the limiting H_2O_2 concentrations at which flames above the liquid extinguish themselves. Here liquid temperatures were low and the burning rate was accelerated by heat transfer from the hotter walls to the liquid. The actual flame temperatures for these runs was presumably higher than that calculated from assumption of adiabaticity, so the points should be displaced to the left. The over-all correlation encourages belief that extrapolation of the correlating line is likely to be valid beyond the range of data in this work.

The similar plot of Semenov's first order expression (equation 10) has a slope similar to that of Figure 8. Separate lines are obtained from the liquid and from the vapor data, as the liquid data are displaced greatly by the effect of the third power of the flame temperature.

The only reported attempt found in the literature to correlate liquid with vapor decomposition data was made by Adam and Stocks (1) for the hydrazine decomposition flame. They obtained a curve from a Semenov first order expression for the vapor data and their liquid data fitted on an extension of this curve. This flame reaction was

Ceckler's burning velocities are slightly higher at lower concentrations and lower at higher concentrations.

One possible cause for the variation of Ceckler's burning velocities with position is that, unlike this work, his burner tubes also served as superheaters and also vaporizers of any entrained liquid drops in the vapor. Consequently some turbulence was probably present although he assumed laminar distribution of vapor velocity in calculating the burning velocity. The fact that he usually found an increase in his calculated burning velocity in the direction of the tip of the flame strongly suggests that some turbulence was actually present, which would cause a flatter velocity profile than that assumed.

Ceckler was able to propagate flames at the tip of the same size of tubes as were used in this work, at concentrations below those where quenching at the tube top prevented propagation here. This indicates a higher temperature of the walls of the tube than he reported, which made it possible to overcome the quenching effect at those concentrations.

CORRELATION WITH QUENCHING DISTANCE

Potter and Berlad (30) derived a relationship between quenching distance and burning velocity based on Semenov's equations. They found that the product of the burning velocity and the quenching distance is a complicated function of transport properties. They also found empirically that the above product term is a simple function of initial gas temperature, flame temperature and pressure of the form:

$$Sd_q \propto \frac{T_o T_f}{P} \qquad (12)$$

This correlation for a number of hydrocarbon-oxygen-nitrogen flames is plotted in Figure 9.

Marshall (25) studied the quenching distance of H_2O_2 - H_2O vapor mixtures, containing between 35 and 50 mole percent H_2O_2, at pressures between 25 and 200 mm Hg. He correlated the values he found for quenching distance by the equation:

$$\log_{10} d_q = 4.362 - 9.360y' + 6.80y'^2 - 0.835 \log_{10} P \qquad (13)$$

Where P is in mm mercury. Values of quenching distance for H_2O_2 vapor mixtures, for the range of data in this study, were extrapolated by means of equation 13 and were used to correlate the data of this work. The results are given in Table V and are plotted in Figure 9.

Despite the scatter in the data there is a definite correlation. The correlating line does not go through the origin. A similar plot for hydrogen-air flames (7) had to introduce a modification in the form of a concentration term to allow for the large effect of hydrogen concentration on the transport properties of that system. Similarly for H_2O_2 - H_2O vapor the different effect of concentration on transport properties and flame properties is likely to

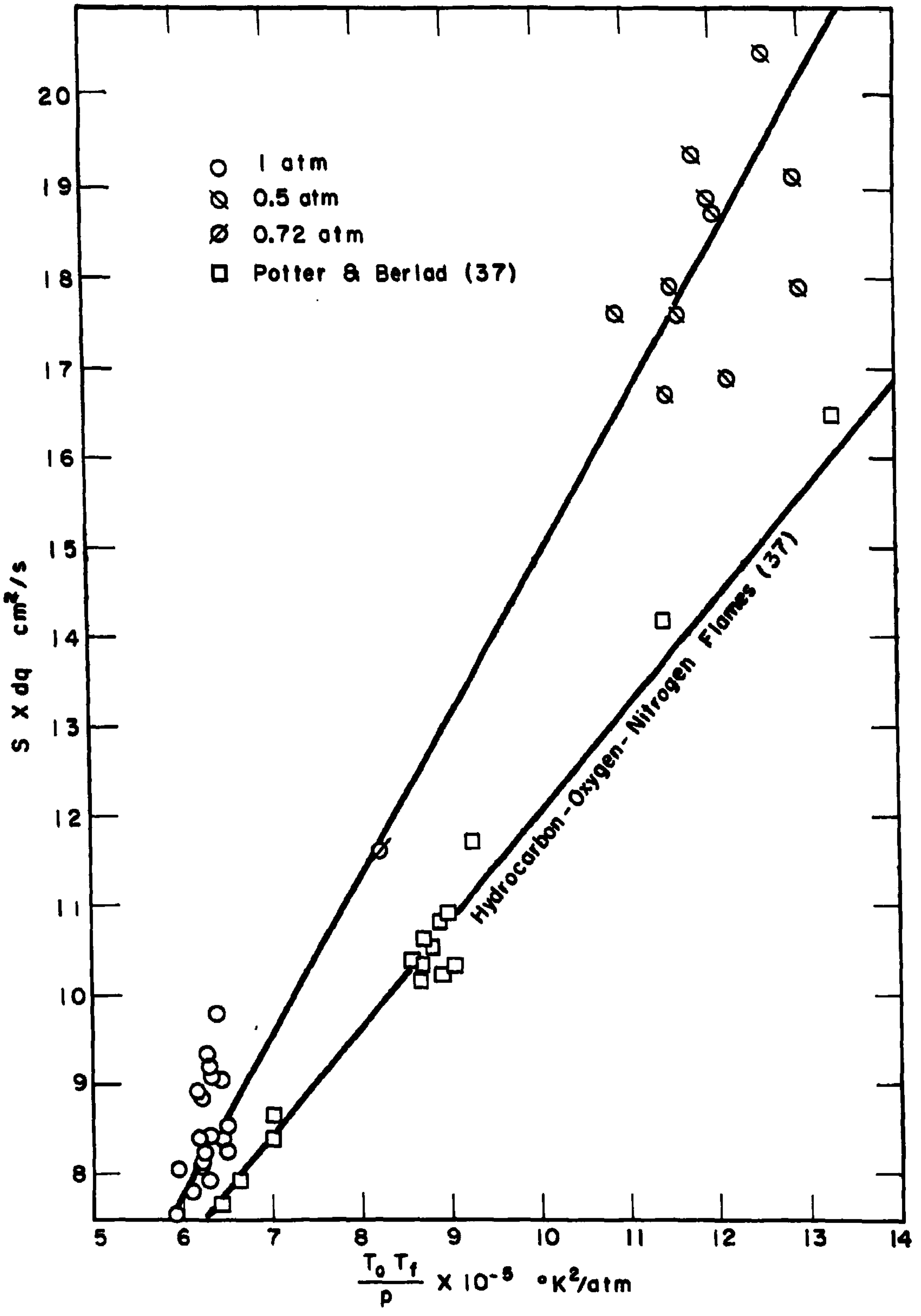

FIG. 9 CORRELATION OF BURNING VELOCITY AND QUENCHING DISTANCES

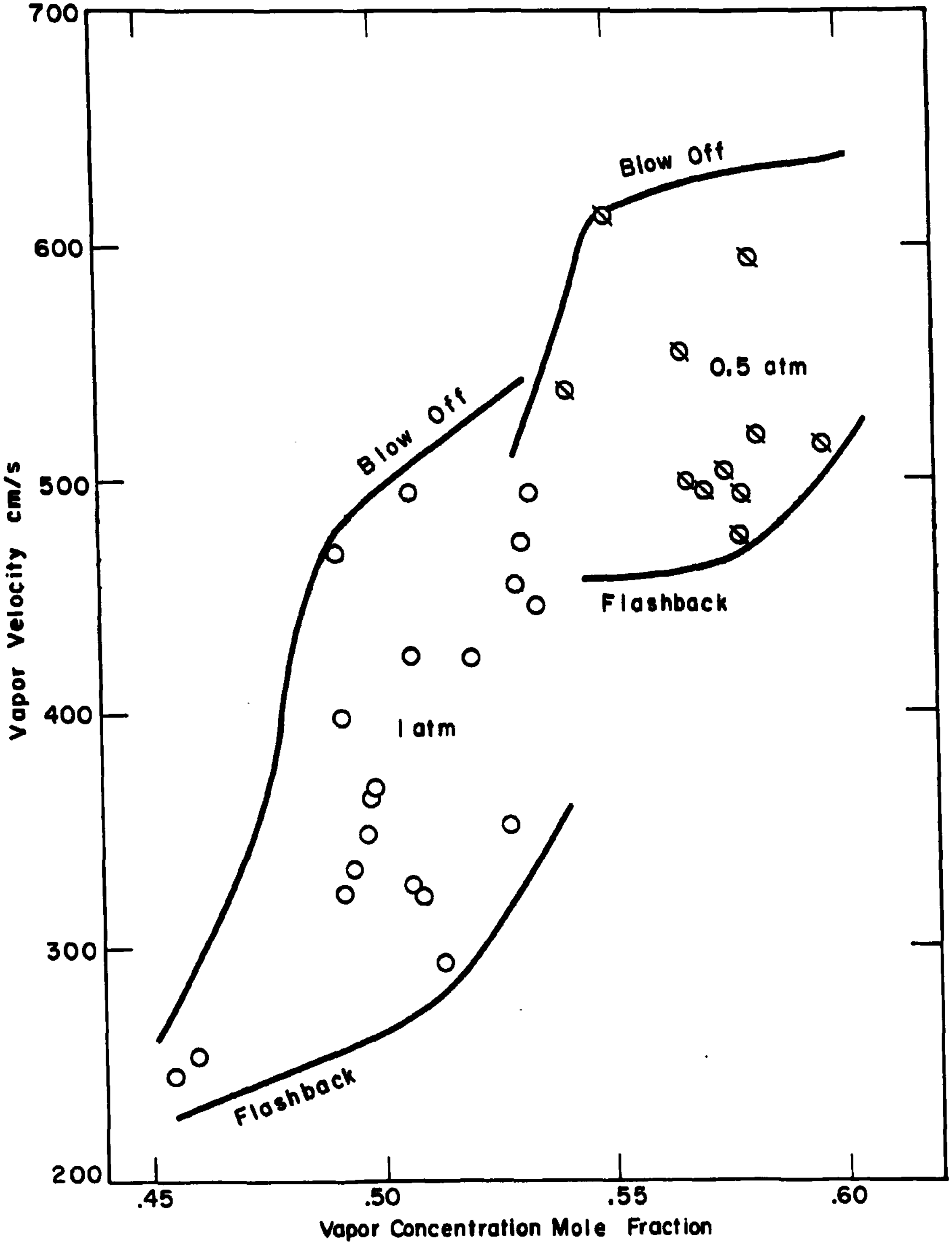

FIG. 10 APPROXIMATE BLOW-OFF AND FLASHBACK LIMITS

ranges should be lower, i.e. the slope of the lower part of the curves should have the same form as the slope of the upper part of the curves for flashback in Figure 10.

E. Table of Nomenclature

Cp - heat capacity of species or mixture (cal/mole °K)

$\overline{Cp}$ - average heat capacity of mixture for T_o-T_f (cal/mole °K)

d_q - quenching distance (cm)

E - apparent activation energy (kcal)

k - constant

n - order of reaction

P - pressure (at)

R - gas constant

S - burning velocity (cm/s)

T - temperature (°K), T_f - flame temperature

y - mole fraction of H_2O_2

Δ Hc - heat of decomposition of H_2O_2 vapor (cal/mole)

α - proportionality symbol

ρ - density of vapor (mole/cm^3)

λ - thermal conductivity (cal/s cm °K)

Subscripts

o - initial

f - final

Literature Citations

1. Adams, G. K., and Stocks, G. W., Fourth Symp. on Combustion, p. 239, Williams and Wilkins, Baltimore, 1953.

2. Baulknight, C. The Calculation of Transport Properties at Elevated Temperatures. General Electric Rept. R 58 SD 223, (1957).

3. Berlad, A. L. and Potter, A. E., Comb. & Flame 1, 127, (1957)

4. Ceckler, W., The Decomposition Flame of Hydrogen Peroxide Vapor. Sc. D. Thesis in Chem. Eng. M.I.T. (1960)

5. Clingman, W. H. and Pease, R. N., J. Am. Chem. Soc. 78, 1775. (1956)

6. Culshaw, G. W. and Garside, J. E., Third Symp. on Combustion, p. 204. Williams and Wilkins, Baltimore, 1949.

7. Drell, I. L. and Belles, F. E. Survey of Hydrogen Combustion Properties. NACA RM E57D24. (1957)

8. Fenn, J. B. and Calcote, H. F., Fourth Symp. on Combustion, p. 231. Williams and Wilkins, Baltimore, 1953.

9. Forst, W., Can. J. Chem. 36, 1308. (1958)

10. Freidman, R. and Burke, E. Fifth Symp. on Comb. p. 596. Reinhold, New York, (1955)

11. Fristrom. R. M., J. Chem. Phys. 24, 888. (1956)

12. Gerstein, M., Fourth Symp. on Combustion, p. 35. Williams and Wilkins, Baltimore, 1953.

13. Gerstein, M., McDonald, G. E. and Schalla, R. L., Fourth Symp. on Comb., p. 375. Williams and Wilkins, Baltimore, 1953

14. Gibbs, G. J. and Calcote, H. F., J. Chem. and Eng. Data 4, 226. (1959)

15. Giguère, P. A. and Liu, I. D., Can. J. Chem. 35. 283. (1957)

16. Gray, P. and Lee, J. C., Sixth Symp. on Combustion, p. 255. Reinhold, New York, 1957.

17. Grove, J. R., Hoare, M. F. and Linnet, J. W., Trans. Farad. Soc. 46, 745, (1950)

18. Hilsenrath, J. Editor. Tables of Thermal Properties of Gases. Circ. United States Bureau of Standards No. 564. (1955)

19. Hoare, [illegible]. E., Protheroe, J. B. and Walsh, A. D., Trans. Farad. Soc. 55, 548. 1959.

20. Kaskan, W. E., Sixth Symp. on Combustion, p. 134. Reinhold, New York, 1957.

21. Keyes, F. G., Trans. A.S.M.E. 77, 1395, (1955)

22. Keyes, F. G., Trans. A.S.M.E. 73, 589, (1951)

23. Lewis, B. and Von Elbe, G., J. Chem. Phys. 11, 75, 1943.

24. Manton, J. and Millikan, B. B., Proc. Gas Dynamics Symp. on Aerothermochemistry, p. 151. Northwestern University, (1956)

25. Marshall, J. G., Trans. Farad. Soc. 55, 288. (1959)

26. McLane, C. K., J. Chem. Phys. 17, 379. (1949)

27. Mendes, M. A. T., Decomposition Flame Above Liquid Hydrogen Peroxide. M.S. Thesis in Chemical Engineering, M.I.T. (1957)

28. Penner, S. S. and Crowe, T. H., Proc. Gas Dynamics Symposium on Aerothermochemistry, p. 113, Northwestern University, (1956)

29. Perry, J. H. Chemical Engineering Handbook. McGraw Hill, New York, 1950.

30. Potter, A. E. and Berlad, A. L., A Relation Between Burning Velocity and Quenching Distance. NACA TN 3882, (1956)

31. Reid, R. C. and Sherwood, T. K., The Properties of Gases and Liquids. McGraw Hill, New York, 1958.

32. Satterfield, C. N., Kehat, E. and Mendes, M. A. T., Combustion and Flame 4, 99, (1960)

33. Satterfield, C. N. and Stein, T. W., J. Phys. Chem. 61, 537, (1957)

34. Satterfield, C. N. and Stein, T. W., Ind. Eng. Chem., 49, 1173, (1957)

35. Satterfield, C. N., Wentworth, R. L. and Demetriades, S. T., J. Am. Chem. Soc. 76, 2633, (1954)

36. Schumb, W. C., Satterfield, C. N., and Wentworth, R. L. Hydrogen Peroxide. Reinhold, New York, 1955.

37. Semenov, N. Theory of Normal Flame Propagation. Translated in NACA Tech. Mem. 1026, (1942)

38. Shuler, K. E., Fifth Symposium on Combustion, p. 56. Reinhold, New York, 1955.

39. Singer, J., Grumer, J. and Cook, E. B. Gas Dynamics Symposium on Aerothermochemistry, p. 139. Northwestern University, 1956.

40. Strauss, W. F. and Edse, R., Seventh Symposium on Combustion, p. 377. Butterworths, London, 1959.

41. von Karman, T. and Penner, S. S., "Fundamental Approach to Laminar Flame Propagation" in "Selected Combustion Problems". Butterworths, London, 1954.

TABLE III

Some Theoretical Correlations of Burning Velocity Data.

Run	Group A	Group B	$S^2P\cdot10^{-3}$ cm^2atm/s^2	Group C	Group D	Group E	$10^4/T_f$ $°K^{-1}$
191	21.5	32.6	10.67	6.23	1.52	5.44	6.613
208	21.8	32.7	10.78	6.34	1.56	5.50	6.667
252	6.2	8.8	3.66	2.27	.61	1.95	7.047
254	8.9	12.7	4.29	2.66	.71	2.28	7.007
255	13.5	20.0	6.64	3.95	.98	3.52	6.725
289	19.3	28.6	8.54	5.61	1.30	4.98	6.729
290	15.0	22.2	7.36	4.37	1.11	3.78	6.765
294	14.8	22.0	7.31	4.35	1.08	3.76	6.716
295	17.8	26.7	8.74	5.35	1.33	4.69	6.757
319	22.8	35.2	11.60	6.61	1.57	5.78	6.481
323	15.8	23.7	7.74	4.58	1.13	3.99	6.667
325	21.0	31.5	10.42	6.18	1.51	5.25	6.667
327	12.1	17.7	5.82	3.50	.90	3.01	6.836
335	21.6	33.3	10.90	6.26	1.48	5.48	6.477
352	18.5	27.3	8.39	4.92	1.28	4.24	6.776
358	13.9	20.6	6.89	4.08	1.03	3.52	6.752
359	19.8	30.3	10.02	5.81	1.39	5.07	6.514
363	26.4	40.2	13.25	7.55	1.86	6.58	6.570
367	25.4	39.0	12.88	7.42	1.77	6.48	6.502
368	21.8	33.6	11.01	6.32	1.51	5.52	6.493
382	25.0	72.6	11.21	7.49	3.29	6.58	6.448
383	24.6	68.0	11.22	7.55	3.19	6.63	6.503
384	28.5	82.9	12.56	8.29	3.40	7.34	6.300
385	33.5	101.5	15.56	10.24	3.72	9.09	6.268
386	31.8	93.0	14.73	9.79	4.23	8.65	6.352
387	38.5	83.4	13.10	8.75	3.69	7.73	6.344
389	31.4	94.5	14.53	9.51	4.05	8.44	6.281
390	32.0	101.0	17.65	11.55	5.11	10.25	6.260
391	27.6	90.0	13.15	8.46	3.72	7.55	6.185
394	27.6	90.0	12.66	9.10	4.08	8.07	6.285
397	26.3	80.5	10.56	7.32	3.21	6.48	6.321
399	17.4	35.8	7.55	5.51	1.73	4.78	6.682

TABLE IV

Calculated Values from Data of Mendes (34).

Run	x'	P at.	S cm/s	T_o °K	T_f °K	Cp_f cal/mole °K	λ_f x10^5 cal/s cm°K	S^2P x10^{-3} cm^2 at/s^2	Group F	$10^4/T_f$ °K^{-1}
7	.951	1	25.8	393	1317	10.8	23.5	.666	2.30	7.600
11	.950	1	28.5	396	1323	10.8	23.5	.812	2.71	7.560
12	.958	1	23.3	393	1320	10.8	23.6	.543	1.87	7.576
13	.958	1	28.2	390	1315	10.8	23.6	.795	2.80	7.604
14	.960	1	24.0	391	1318	10.8	23.7	.576	2.01	7.590
15	.870	1	15.9	388	1193	10.4	21.7	.253	1.16	8.380
17	.355	1	16.2	388	1180	10.3	21.3	.262	1.24	8.475
18	.830	1	14.25	390	1127	10.2	21.1	.203	1.05	8.87
19a	.728	1	9.3	405	1013	9.8	19.9	.087	.494	9.87
20a	.740	1	11.6	405	1097	9.8	20.0	.135	.635	9.115
21	.938	1	33.4	398	1317	10.7	23.2	1.120	3.75	7.600
23a	.946	1	44.8	412	1347	10.7	23.4	2.010	5.91	7.425
23b	.928	1	33.6	412	1307	10.7	23.0	1.129	3.47	7.65
24a	.950	1	32.3	399	1325	10.8	23.5	1.043	3.41	7.55
24b	.968	1	32.4	399	1327	10.9	23.8	1.050	3.48	7.535
25a	.950	1	37.1	396	1324	10.8	23.5	1.376	4.55	7.555
25b	.927	1	37.1	396	1292	10.7	23.4	1.376	4.73	7.74
28	.970	1	32.1	387	1326	10.9	23.8	1.030	3.44	7.54
29a	.810	1	26.1	394	1128	10.2	20.8	.681	2.61	8.145
29b	.712	1	21.9	405	990	9.7	19.7	.480	2.95	10.10
3	.770	.526	21.9	379	990	10.0	18.1	.243	2.06	10.10
6	.825	.526	26.8	390	1050	10.2	19.8	.378	2.56	9.52
7	.890	.526	41.2	394	1224	10.6	21.8	.898	3.72	8.17
8	.955	.526	72.0	394	1330	10.9	23.9	2.73	8.89	7.52
16	.940	.526	50.3	388	1307	10.7	23.4	1.334	4.78	7.65
11	.905	.265	50.0	375	1225	10.4	22.1	.658	3.14	8.16
12	.965	.263	65.5	376	1335	10.7	23.6	1.128	4.19	7.49
15	.954	.263	65.6	376	1300	10.7	23.3	1.133	4.44	7.69
13	.970	.131	93.2	335	1295	10.7	23.3	1.139	5.92	7.72

TABLE V

Correlation of H_2O_2 Burning Velocities with Quenching Distance.

Run	S cm/s	d_q cm	$S\ d_q$ cm^2/s	$T_oT_f/P\cdot10^{-5}$ $°K^2/atm$
191	103.3	.088	9.09	6.34
208	103.8	.090	9.34	6.28
252	60.5	.125	7.56	5.91
254	65.5	.123	8.05	5.95
255	81.5	.096	7.83	6.21
289	92.4	.096	8.86	6.21
290	85.8	.098	8.41	6.18
294	85.5	.096	8.22	6.22
295	93.5	.090	8.42	6.29
319	107.7	.077	8.28	6.48
323	88.0	.090	7.93	6.28
325	102.1	.090	9.19	6.28
327	76.3	.102	7.79	6.10
335	104.4	.079	8.25	6.48
352	91.6	.098	8.99	6.18
358	83.0	.097	8.06	6.20
359	100.1	.081	8.11	6.21
363	115.1	.085	9.78	6.38
367	113.5	.080	9.06	6.44
368	104.9	.080	8.38	6.45
382	145	.123	17.81	11.52
383	142	.124	17.60	10.91
384	152	.110	16.71	11.45
385	172	.109	18.73	12.00
386	167	.116	19.38	11.81
387	156	.113	17.61	11.60
389	166	.114	18.90	11.95
390	187	.112	20.92	12.54
391	163	.110	17.92	12.97
394	161	.119	19.13	12.92
397	147	.115	16.90	12.14
399	102	.114	11.62	8.22

Values of quenching distance (d_q) were extrapolated from data of Marshall

TABLE VI

Some Calculated Properties of the Vapor Mixtures.

Run	$\lambda_f \times 10^5$ cal/cm s°K	$\overline{Cp}$ cal/mole°K	Cp_f cal/mole°K	M'
191	27.3	9.61	10.81	.868
208	27.2	9.61	10.80	.867
252	25.5	9.58	10.68	.858
254	25.6	9.58	10.69	.854
255	27.0	9.61	10.78	.865
289	27.0	9.61	10.78	.864
290	26.8	9.60	10.76	.863
294	27.0	9.61	10.78	.865
295	27.2	9.61	10.80	.867
319	27.8	9.63	10.86	.874
323	27.2	9.61	10.80	.867
325	27.2	9.61	10.80	.867
327	26.4	9.60	10.74	.860
335	27.8	9.63	10.86	.874
352	26.8	9.60	10.76	.862
358	26.9	9.61	10.76	.863
359	27.6	9.63	10.84	.872
363	27.5	9.62	10.83	.870
367	27.7	9.63	10.85	.873
368	27.7	9.63	10.85	.873
382	28.0	9.62	10.84	.879
383	27.8	9.61	10.82	.876
384	28.5	9.65	10.89	.885
385	28.6	9.65	10.91	.887
386	28.3	9.64	10.87	.883
387	28.3	9.64	10.88	.883
389	28.5	9.65	10.90	.887
390	28.6	9.65	10.91	.888
391	28.9	9.67	10.94	.891
394	28.5	9.65	10.90	.886
397	28.4	9.64	10.88	.884
399	27.2	9.59	10.79	.868

VIII APPENDIX

A. Tables of Data and Calculated Results.

The following groups are from Tables III and IV.

TABLE III

Group A	$S^2P\,\overline{Cp}/T_o^2\lambda f\cdot 10^{-3}$	cm^3atm/s mole $°K^2$
Group B	$S^2Tf\,\overline{Cp}/T_o^2\lambda f\cdot 10^{-5}$	cm^2/s mole °K
Group C	$S^2Py'^2/T_o^2Tf^3(2+y')Cpf\,\lambda f\cdot 10^{10}$	cm^3atm mole/s $cal^2°K^3$
Group D	$S^2y'^2/T_o^2\,Tf^4(2+y')^2Cpf^2\,\lambda f\cdot 10^{13}$	$cm^3mole^2/s\ cal^3°K^3$
Group E	$S^2Py'^2M'/T_o^2Tf^3(2+y')Cpf\lambda f\cdot 10^{10}$	cm^3atm mole/s $cal^2°K^3$

TABLE IV

Group F	$S^2Px'^2/T_o^2T_f^3\lambda_fCp_f(2+x')\cdot 10^{10}$	cm^3atm mole/s $cal^2°K^3$